milliCTI

Thuso Simon
University of New Mexico Physics and Astronomy
Honors Thesis
May 16, 2008

Thuso Simon
05/16/2008

1. Introduction

For centuries the quest for higher precision measurements has driven astronomers to develop new techniques and design new instruments that yield more information about the physics of the universe. The foremost obstacle that astronomers face when observing the night sky (at optical and infrared wavelengths) is the Earth's atmosphere, which both blurs images and blocks light. With the advent of the space age, we have been able to place telescopes in orbit, well above the atmosphere's influence. However, this method of obviating the atmosphere is very expensive. The next best step is to make a ground-based telescope that reaches for high levels of photometric and astrometric precision only previously achieved from orbit, while simultaneously measuring everything about the atmosphere. The CCD Transit Instrument with Innovative Instrumentation (CTI-II) project is doing that by creating new and innovative ways to minimize the effects of the atmosphere by equipping the existing CTI telescope with modern optics, new telescope structure and detectors while developing new techniques and instruments to better quantify the observatory environment. Not only will it create and test new ways of accurately measuring the atmosphere, but it will also help astronomers map out the sky and create new astronomical standards that all astronomers can use for their own measurements.

CTI-II will be discussed in more depth in Section 2. The designing process and construction of milliCTI (mCTI), is detailed in Section 4. Section 5 will cover how to operate and collect data with mCTI. Section 6 recounts the observations and Section 7 details the programs that were used to reduce the data and the data reduction processes. In section 8, we discuss the results from mCTI and a summary and future work for mCTI is presented in section 9.

Section 3 covers the first of the auxiliary instruments designed to quantify the atmospheric extinction, the Astronomical Lidar for Extinction (ALE). One of the innovative techniques being developed at UNM is ALE. ALE will quantitatively measure the extinction of the atmosphere, which gives astronomers real-time, accurate data about astronomical extinction. My research project is to verify and calibrate the accuracy of ALE. Once this method of calibration is developed, it can be used to help future telescopes trust and use Lidar systems.

2. CTI-II

CTI-II is a 1.8m transit telescope, currently in development at the University of New Mexico. Using Time Delay and Integration (TDI) readout mode, which will be described in more detail in later in this paper, CTI-II images at a constant declination, letting the Earth's rotation sweep out a 1° wide strip in declination that is about 120° (8 hours) long in right ascension each clear night [4]. Much of this area will be overlapping from night to night because of the Earth's orbital motion around the Sun which advances the strip by 1° per night. Over the course of a year, it will cover an entire small circle of the sky at 28° declination. This allows comparison of the sky between nights to find changes in the sky. Over the course of its operation, CTI-II will observe millions of stars and hundreds of thousands of galaxies. A large fraction of these will change in some way, whether they are variable stars, AGN, high proper motion objects, supernovae or even a previously unknown class of object, all of which are of great interest in astronomy [1]. But even stars that don't vary are also interesting (albeit to a somewhat different subset of astronomers) as they are good candidates to become standard stars upon which other measurements are based. As with other telescopes, the observatory environment and intervening atmosphere wreak havoc with the accuracy and precision of the measurements CTI-II could otherwise produce.
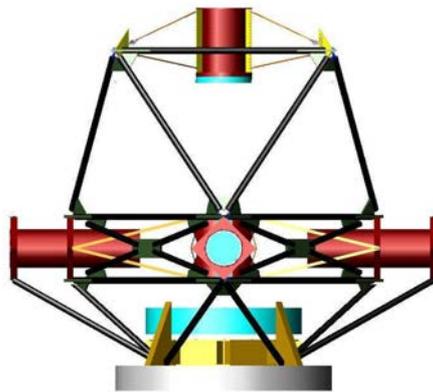

Figure 2.1

Front view of CTI-II's CCD array and primary mirror

The CTI-II telescope has many innovations that will help it reach its goal of sub-1% photometry and milliarcsecond astrometry. One of these innovations is to have CTI-II constantly pointing near zenith which gives the telescope a constant gravity load, enabling a stable optical platform [1]. The telescope structure is designed to compensate for the differences in temperature due to seasonal and diurnal variations without losing focus or pointing. To do this the structure uses materials with complementary thermal properties so that when the ambient temperature changes, the telescope keeps it alignment. The latest design for CTI-II's structure consists almost entirely of carbon fiber tubing. Not only are carbon fibers relatively easy to make athermal, but they will also come to ambient temperature faster than steel or aluminum [1].

The thermal load of the telescope structure and enclosure is a big issue preserving the natural turbulent environment of the observing site. Many older research telescopes have a large thermal mass in the telescope and its enclosure, making the telescope take a long time to come into equilibrium with the free air. This can cause convection currents, called 'dome seeing,' that are created from this lack of homogeneity in temperature, which degrades the optical performance. But thermally induced dome seeing and thermal deformations of the telescope structure are not the only ways the atmosphere can interfere with the fidelity of a telescope's measurements [1].

3. Astronomical LIDAR for Extinction

The atmosphere can cause what astronomers call "atmospheric extinction," a wavelength dependent scattering and absorption of the incoming light from stars and galaxies. Another major problem from the atmosphere comes from the molecules and other particles that it is made from. Studies on the transmittance of the atmosphere show that extinction can come from at least four categories of sources. First there is molecular absorption. It comes from the molecules in our atmosphere like water, O_2, O_3, etc... The extinction caused by molecular absorption can be highly variable and is not very well modeled [2]. Ozone, for instance, completely absorbs wavelengths in the ultraviolet part of the spectrum [3]. The next source of extinction can come from molecular scattering, also known as Rayleigh scattering, which is proportional to $\frac{1}{\lambda^4}$. This happens from the molecules that are most abundant in the atmosphere like N_2 and O_2, and the extinction varies from this source very slowly with atmospheric pressure.

Clouds are the extreme case of molecular scattering. They consist of either liquid droplets (cumulus, etc.) or ice crystals (cirrus). The droplets or crystals are much bigger that the wavelength of visible light, so they scatter in a wavelength independent manner. This means that they don't absorb visible light; they scatter all visible wavelengths evenly and can be highly variable [2]. Lastly there are aerosols, particles aloft such a soot, smoke, smog, and dust, which have sizes comparable to the wavelength of visible light. Scattering from aerosols is in the Mie scattering regime and scales roughly as $\frac{1}{\lambda}$, but is complicated by the variety in sizes of aerosol particles even within a given type of aerosol. More often than not, multiple types of aerosols will be present in varying ratios and can change seasonally and even on time scales as short as 15 minutes [3]. The absorption properties of aerosols are also complex and difficult to model [2].
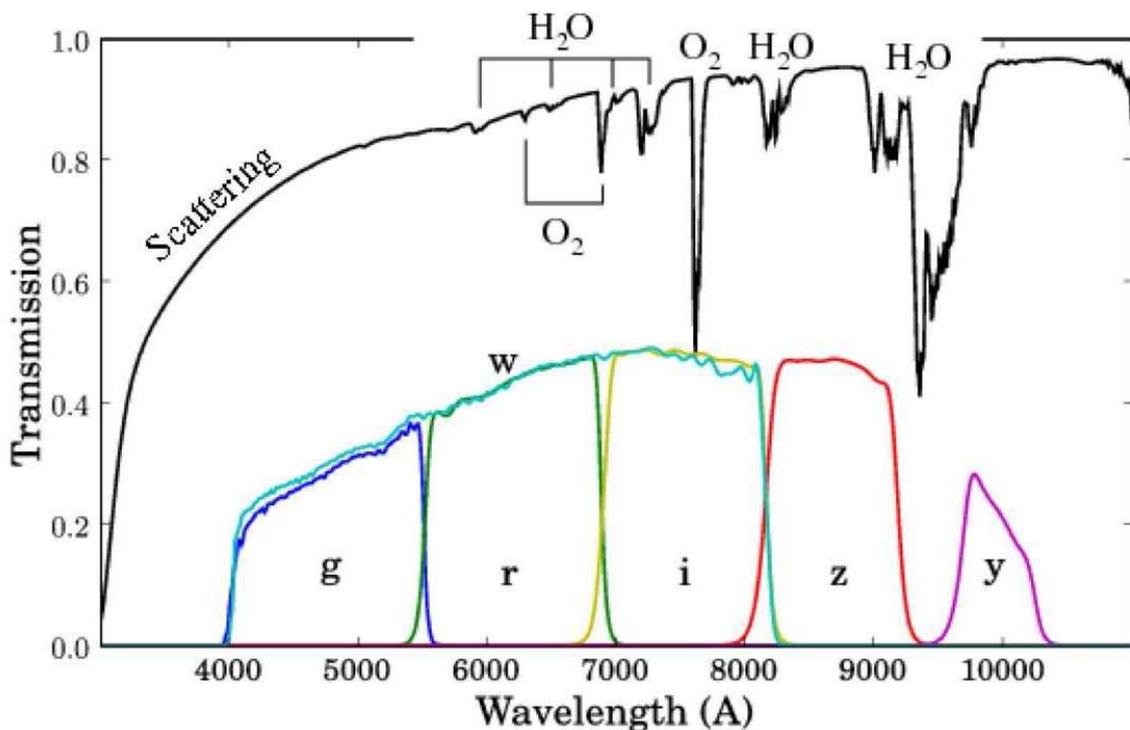

Figure 3.1

Transmission through the Atmosphere looking at Zenith [4]

The most common methods that astronomers currently use when photometric precision is required to correct for atmospheric extinction are estimates averaged through the night. In some cases average seasonal values are used. In order to get enough measurements of the changes in atmosphere over a reasonable time frame, astronomers would use too much precious telescope time that could otherwise be spent observing the objects that they are interested in measuring.

Many efforts are ongoing to obtain more accurate and precise measurements of atmospheric extinction. We can see in Figure 3.1, one groups [4] measurement of the transmission of the atmosphere and the quantum efficiencies of their CCD's (g,r,I,z,and y). Many of these groups however, are using their atmospheric measurements for fields of science other than astronomy.

Independent systems dedicated solely to measuring extinction are being developed for deployment at major observatories to help address this problem. One such effort is the Astronomical LIDAR for Extinction (ALE), a project currently undergoing integration and calibration testing at the University of New Mexico's Campus Observatory. ALE will give real time data about the extinction of the sky in 1-minute intervals to better than 1% at 527 nm [5].

ALE is a LIDAR (Light Detection And Ranging) system that works in a way analogous to RADAR but with visible light instead of radio waves, by transmitting eye-safe 527 nm laser pulses into the night sky. When the photons from the laser encounter molecules or particulate matter, some photons will scatter. If the photon happens to backscatter at the right angle, the detector of ALE, a .67m telescope with a photomultiplier detector, will observe it. Once the photon is observed, ALE will calculate the altitude by using a simple time-of-flight measurement for the round trip travel time for the pulse traveling at the speed of light. The photomultiplier records a 15m resolution atmospheric profile for each pulse it transmits from ground level up to 60km, where the number of returned photons at a given altitude is related to the density and scattering properties of the material there as well as the atmospheric transmission to and from it. The real leverage of ALE that enables high precision atmospheric monitoring is that it acquires 1500 profiles per second [5].

The profiles measured by ALE are governed by the so-called Lidar equation, which is commonly written:

$$p(R) = p_0 \cdot \eta \left(\frac{A}{R^2}\right) \cdot \left(\frac{c \cdot \tau}{2}\right) \cdot \beta(R) e^{-2 \int_0^R \alpha(r) \cdot dr}$$

where:

$p(R)$ is the signal from the lidar at altitude R,

p_0 is the transmitted power,

η is the detector efficiency,

A   is the receiver area,

R   is the range from the Lidar source to the scattering volume,

c   is the speed of light,

τ is the sampling interval,

β is the atmospheric backscattering coefficient,

α is the atmospheric extinction coefficient [5].

In order to make an accurate measurement of the transmittance of the atmosphere, the atmosphere is modeled to be homogenous and free of aerosols and clouds [6]. With this model, ALE should detect 10^6 photons per minute from a 20-40 km range from ALE. Unfortunately, the lower 20 km is not free of aerosols or clouds and is where most of the extinction in the atmosphere happens. ALE detects less photons per minute at the 20-40 km range depending on the transmission of the lower atmosphere. By using different lines of sight, between $0°$ and $60°$ from zenith [5], ALE is able to calculate the transmission of the atmosphere. ALE can also measure the altitude of the aerosols and clouds by using the time of flight from the backscatter off these particles.

Because it is a new instrument and the technique is new to astronomers, ALE's ability to measure atmospheric extinction must be assessed at UNM's Campus Observatory. Therefore, some other means of independently assessing extinction is needed that can be compared with ALE measurement of the extinction.

4. milliCTI

For this project I built a wide field, 525nm narrowband photometer, the aperture of which is about a thousand times less collecting area than CTI-II, to help calibrate ALE. The reason we chose to build a small instrument for calibrating ALE is because milliCTI (mCTI) would be easy to deploy, it is simple to operate and it is inexpensive. With the design we also had to make sure that mCTI would be able to attain the sub-1% photometry goal.

mCTI was also designed to run without a mechanical tracking system, like CTI-II and operate in TDI mode. The way TDI works is by letting the CCD array do the tracking while the telescope stays still clocking out the pixels at the same rate that the stars drift across. Let's say that there is an astronomical object occupying pixel "n" on a CCD array; as the object moves across the sky in its diurnal motion it will also move across the CCD array. The objective of TDI mode is for pixel "n" to shift with the object as it moves across the array. When the object reaches the end of the CCD array, pixel "n" will be digitized and stored without having to close the shutter of the camera. The advantages and disadvantages of this method of collecting images will be explained more in depth later in the thesis.

4.1 Design

In order to keep mCTI measurement error below the 1% goal of this project, I tried to implement as many of the precision photometric methods outlined in Stubbs and Tonry's paper on the topic [7].

I.   Flat Fielding

Having a design that could be easily flat fielded was an important concern. In a normal CCD, there are pixels that can have greater or lesser efficiency than the other pixels in the CCD array. This can also be compounded by the optics of the telescope not uniformly illuminating the CCD [2]. To compensate for this effect a flat field is applied to the image. The flat field is acquired by taking an image of a uniformly illuminated object. This

object will illuminate the CCD, evenly showing the sensitivity of each pixel. To make sure that the flat field is precise, the average number of photons per pixel received by the CCD should be enough that the signal to noise ratio is high (for 1%, signal to noise should be greater than 300). To apply the flat fields to the images, one subtracts the dark exposure (an equal time exposure with shutter closed) from the flat field, then takes that result and divides that corrected flat field from each image. Using flat field corrections is not really a design that could be built into mCTI, but flat fields are used in data reduction process.

II.   Reduction of Optical Bandwidth

In order to implement this I needed to build my telescope with a filter. ALE measures extinction at 527 nm, so mCTI should work around the same wavelength. Keeping the bandwidth around ALE's also keeps mCTI from experiencing too much wavelength dependent extinction due to most molecular absorption.

III.   Determine the Throughput of the Imaging System

To accomplish this I needed to use imaging components that have well known throughput properties associated with them. By knowing the exact materials that make up the lens, the bandpass of the filter, and the quantum efficiency of the CCD, I should be able to account for the throughput of the system. Most importantly though, is that it does not change over the course of my experiment. If it does change, it should change over the course of months or years, not days.

IV.   Design telescopes that are easy to calibrate

By designing mCTI to be as simple as possible, I have cut down on as much systematic error as possible. By using the correct software programs

for acquiring and analyzing the data I collect, I should be able to drastically simplify my calibration process.

Keeping in mind the goals listed above, mCTI also was made to be light and compact. This will cut down on the cost of the telescope and make it easily transportable when more instruments like ALE start being built for use at other observatories.

 The optical system of mCTI has a 150 mm achromatic doublet lens as the objective, which is held in place by its focuser. The focuser also holds in place the 527nm, 30 nm wide filter. The focuser then screws directly into the CCD camera, an SBIG ST-402ME. The properties of the CCD are shown in Table 4.1. The telescope is then bolted to a mount which keeps the telescope pointing in the same direction. We chose to have the telescope pointing at zenith every night so that it would be easy to know the coordinates at which the telescope was pointing. Originally the telescope was designed to run in TDI mode; after some considerations, which will be discussed later, it was made to run in the normal exposure mode even though it doesn't track.

Camera	Pixel Array	Number of Pixels	Pixel Size µm	CCD Size mm	CCD Area mm^2	Read Noise	Full Well Capacity	Full Frame Transfer
ST-402ME	765 x 510	390,000	9	4.6 x 6.9	32	17e$^-$	100,000 e$^-$	0.8 sec

Table 4.1

Properties of ST-402ME [8]

4.2 Theoretical Calculations of mCTI

Before buying most of the parts to build mCTI, I calculated the signal to noise values that could be expected for different magnitude stars and for the different focal lengths of lenses. These calculations were made from data sheets made available by vendors. To calculate these values I assumed that the flux of photons coming from a 0th magnitude star is 9.6×10^{10} photons per meter^2 per second per unit bandwidth of filter. The total transmittance of photons from astronomical sources to my CCD chip was 17.6% which is a decent intermediate value. This value comes from a conservative assumption that the transmittance of the atmosphere is 80%, the transmittance to

the optics in the telescope is 40% and the quantum efficiency of the CCD itself was 55% at 530 nm. To calculate the cross time across the CCD I used the simple lens formula:

$$t = \frac{206265 \cdot d}{f \cdot \omega \cdot \cos(\delta)}$$

where f is the focal length of the lens, ω is the angular rotation speed of the earth, d is the crossing length of the CCD and δ is the declination of the telescope.

Focal Length (mm)	Time for Image to Cross CCD (Seconds)
50	1541.035
100	770.5174
150	513.6783
200	385.2587
250	308.207

Table 4.2

Focal lengths and the respective cross times for the ST-402ME CCD when telescope is not tracking

With these times and the calculated throughput of the telescope, I was able to calculate the estimated signal to noise of different magnitude stars for my telescope.

	focus length (mm)	0	1	2	3	4	5	6	7	8	9	10
Magnitude		**0**	**1**	**2**	**3**	**4**	**5**	**6**	**7**	**8**	**9**	**10**
S/N	50	9.48E+04	2.51E+04	1.58E+04	9.99E+03	6.30E+03	3.98E+03	2.51E+03	1.58E+03	9.91E+02	6.18E+02	3.78E+02
S/N	100	6.71E+04	1.78E+04	9.71E+05	7.07E+03	4.46E+03	2.81E+03	1.77E+03	1.11E+03	6.95E+02	4.28E+02	2.56E+02
S/N	150	5.48E+04	1.45E+04	9.14E+03	5.77E+03	3.64E+03	2.29E+03	1.44E+03	9.05E+02	5.63E+02	3.43E+02	2.00E+02
S/N	200	4.74E+04	1.26E+04	7.92E+03	5.00E+03	7.69E+04	1.99E+03	1.25E+03	7.82E+02	4.84E+02	2.92E+02	1.67E+02
S/N	250	4.24E+04	1.12E+04	7.08E+03	4.47E+03	2.82E+03	1.77E+03	1.12E+03	6.97E+02	4.29E+02	2.56E+02	1.44E+02

Table 4.3

Theoretical calculations of the signal to noise ratio for cross times equal to the cross time through the CCD

From the values in Table 4.3, I had to consider the best way to get the best signal to noise ratio through the components that were available.

4.3 Choosing a CCD

Originally the telescope was going to operate in TDI mode like CTI-II. This idea ran into major problems while building mCTI. The first problem encountered was the availability of a CCD that was made to work in transit mode. The Ascent model 1107 (A1107) and Apogee Ascent model 98 (A98), were both unavailable from the distributor contrary to what their sales team told us. The only option I had left was to use a CCD that was already owned by Dr. McGraw's lab group, the SBIG ST-402ME. This CCD was not made to be used in TDI mode, it was not narrow enough and created smearing, but I tried anyway. The major problem was that in TDI operation the rectangular format of the CCD is projected onto the celestial sphere. This means that the tracks of stars are differentially curved from top to bottom across the CCD. In addition stars near the top of the CCD move at a slower rate than stars near the bottom. The differential rate was calculated and is shown in Table 4.3. The differential drift time is far larger for the SBIG CCD we are required to use than for the unavailable Apogee cameras.

12

Model	Focal Length (mm)	Differential Drift Time (seconds)
Ascent A1107	150	25.96139822
Ascent A98	150	3.475706319
ST-402ME	150	81.39536738

Table 4.3

Differential drift time for the three CCD's available for this project

Because the optics project the celestial sphere onto the CCD, the stars on the northerly portion appear to drift more slowly across the device, as governed by the $\frac{1}{\cos(\delta)}$, the differential drift time is the difference in time it takes a star moving through the center of the CCD relative to time it takes for a star to drift across the outer edge of a CCD pixel array. The declination at the top and bottom of the device is different, and the drift rates are from the rate that the CCD is clocked. The ST-402ME differential drift time is approximately three times greater than the A1107. This drift time caused many problems in using this camera in TDI mode. For this reason the TDI readout mode was abandoned and a measurement mode involving a number of sequential short exposures with respect to the TDI integration time was implemented. The ST-402ME has a 765X510 pixel array where each pixel has a size of 9 μm. The camera can connect to a computer using a USB port.

Figure 4.1

Picture of mCTI build with all of it components

4.4 Filter

The filter was chosen to match the wavelength of ALE, 527 nm, which is the first harmonic of a ND:YLF laser. This is conveniently in the middle of the standard V bandpass. It is also well away from any large molecular absorption band, except a small ozone band which can be seen in Figure 3.1.

Another problem I had with the building of mCTI was with my first filter. It was centered at 527 nm and had a bandpass of 10 nm. This filter had a very narrow bandwidth which made the number of stars I was able to use for my data reduction very small due to low throughput. Also the filter created ghost images, which can be seen in Figure 4.2, were very persistent through my

images. The problem with the filter was that it was made for narrowing bandwidth lasers, and not meant to be used for astronomical imaging.

Figure 4.2

Image of stars with ghost images created by the First Filter

The second filter was made by Chroma Technology Corporation. This filter is the OS03306, which is an interference filter, whom a bandpass centered at 525 nm and a bandwidth of 30 nm. We chose to use this filter with the wider bandwidth so that the signal to noise would be better. It had a few problems as well, and it created an image of the CCD chip when exposed under high light situations. I only encountered a visible ghost image when I was taking my flat fields images during high light situations, but these images are still worrisome. The curious property of these ghost images of the CCD chip was that they would stay in focus no matter how I changed the focus of the lens; the ghost image always stayed the same. This ghost image made it so that I could not apply my flat fields to my images and ruined my chances of achieving my 1% goal. The original placement of the OS03306 was in front of the lens. It was put there so it would be in

plane parallel light, ensuring that the bandwidth of the light was the same as it was specified by the filter. In order to fix the ghost problem I had to move the filter as close to the CCD chip as I could. This change in position would put the filter in converging light which cause the effective bandwidth of the filter to increase by about 5 nm blueward and shift the central wavelength to 527.5 nm. The decision to sacrifice the accuracy of the bandwidth was overridden by the need to get rid of the ghost images. After the change in position of the filter, in high light situations there were no more ghost images.

Figure 4.4

Flat Field exposure with Ghost image of CCD Chip

4.5 Lens

In choosing the best lens for the project, there were many considerations put into purchasing the right one. The lens has to have a high transmittance in the 530 nm range, and produce a good

image over a 10° field of view, which is more than enough for mCTI [9]. The achromatic doublet lens was the best choice because even though mCTI images over a small bandwidth, the achromatic is also constructed to minimize spherical aberrations as well as chromatic aberration [9]. By choosing this lens which has a 150 mm focal length, I was able to achieve my goals in designing the telescope. The combination of the lens, focal length and the size of the CCD gave mCTI a 2.6^ox1.8^o field of view. This large field of view opened up new avenues that the project could take which I will discuss later in the paper.

4.6 Mount

The original motivation of the design of the mount was for it to be easy to align to true north and that it would point at zenith. These two goals were very difficult to achieve in the actual construction of the mount. The first mount that was constructed was a 5"X2' strap of metal that had an adjuster bolted to it. mCTI was then fastened to the adjuster which, without weight, is perpendicular to the ground. When the weight of the telescope was added to it, it causes the telescope not to be pointed exactly at zenith. Aligning this telescope with North was also a challenge. The adjuster, which was supposed to allow for fine adjustments while aligning the telescope with north, caused major problems because the adjuster knob was broken. The adjuster allowed for the telescope's position to be locked in place but didn't move finely when it was in the unlocked position.

The second mount was a much needed improvement to the first one. It is much more stable and points vertically much more accurately. The new mount was 3 square pieces of metal which were sandwiched by springs. The springs allowed me to adjust the flatness of the camera even when it wasn't laid on a flat surface. The upper-most piece contained a metal strap that could hold the telescope to the mount.

5. Running mCTI

In this section the setup, alignment and operation of mCTI is described.

5.1 Setting up mCTI

When observing with mCTI, setting up the telescope is fairly fast. First, I would attach the CCD camera to the mount and bolt the whole thing down. Then I would take the lens and filter setup and screw it onto the camera. Lastly, I would place the telescope on my observing pier, which is a cement block that is about 5' off the ground. I would begin my observations at dusk allowing me to start my observations by taking twilight flat fields.

5.2 Observing with mCTI

I ran mCTI off of a laptop that connected to the telescope with a program called Maxim DL. Maxim recorded the images it took with the standard Fits (.fit) files. After some trial and error with Maxim, I was able to create a script that made the observing completely automatic. First, I had the program take twilight flat fields. Then I took dark exposures and dark current bias frames. After that I started the actual observing of the night sky.

Originally, I had planned on using mCTI in TDI mode. TDI mode has many advantages, for instance, it gets more stars per image due to the longer integration time. This longer integration time also increases the signal to noise of each star allowing for a greater sample of stars per image. However, when I first started to assemble the telescope I ran into problems. The first major problem I encountered was from the differential drift time. An example of the smearing due to the differential drift time can be seen in Figure 5.1. The only solution I could think of without changing the physical components of the telescope was to use a smaller area of the detector for my image. This would cut down the number of stars that I could use which in turn would reduce the total amount of data I could receive.

The second major problem I had with running in TDI mode was aligning the telescope to the North. Since the mount I used for my telescope wasn't very technologically advanced, I had to align it myself. After many nights of practicing in the cold of winter, I finally came up with a relatively fast and accurate method to align mCTI with North. I started by taking a continuous string of images in Maxim every 5 seconds. I started with stars coming into my field of view. I then drew a straight line along the path that the star would drift if the telescope was aligned perfectly north. On the star's 8.5 minute journey across my field of view, if I noticed that the star wasn't traveling exactly along the path, I would realign the telescope and start over with a new star coming into the field of view. The problem in aligning the telescope like this is it still took about an hour to align mCTI, and the accuracy of the star traveling down a straight path was constrained to human error. Because of the human error, there was smearing in the regions where the differential drift time was small. In the end I had to abandon the TDI mode, which actually added more avenues that I could follow with this project.

Figure 5.1

Example of an image taken in TDI mode. Notice the in focus stars in center of image while the outer edges are smeared due to the differential drift time.

After I decided to stop using my telescope in TDI mode, I started testing more pragmatic approaches to data collection. I decided to acquire the photos using the regular exposure mode. I tested for the best exposure length and in the end the exposure time that balanced between the numbers of bright stars vs. the minimum number of stars that were smeared was 5 seconds.

The proof that all of my calculations were close to what I had predicted came after I changed into regular exposure mode. When making the calculations for Table 5.1, I used very conservative estimates for the error. This made the calculated signal to noise lower than the observed. The match to theory was evidence that mCTI was ready to start acquiring real data in this mode.

		Theoretical		Real	
Tycho #	**V mag**	**# Photons**	**S/N**	**# Photons**	**S/N**
Tyc 245902551	7.1	7.42E+03	4.78E+01	6.37E+03	5.74E+01
Tyc 249612231	5.992	2.06E+04	1.07E+02	1.72E+04	1.26E+02
Tyc 245917841	8.86	1.47E+03	1.09E+01	1.37E+03	1.57E+01
Tyc 248921411	5.591	2.98E+04	1.38E+02	3.13E+04	1.84E+02
Tyc 246114641	9.51	8.06E+02	6.09E+00	8.16E+02	8.85E+00

Table 5.1

Theoretical vs. Real Data taken on March 3rd with a 5 second exposure time

6. Data Acquisition

Data were acquired on several nights, leading to the demonstration of the utility of mCTI to accomplish its mission of real-time atmospheric transparency monitoring. All of these data were acquired in 2008 and the dates record civil time at the beginning of an observation.

6.1 February 27

I started taking 5 second exposures simultaneously with ALE at 10:32 pm local time. I aligned mCTI with North and marked the position of the telescope on the observing pier for consistency on later nights. Unfortunately, ALE and mCTI were pointing in the same direction and the Lidar beam was in the field of view of the telescope as can be seen in Figure 6.1. To correct this I moved the field of view 2.5° off zenith along the plane of the equator. Before starting the exposures I took bias and dark exposures. The observing conditions were high clouds and generally hazy sky with the smell of wood burning stoves. The temperature was cold; approximately 30 degrees F. I stopped taking observations at 12:17 AM with the total number of exposures at 1009. During the night the moon didn't rise. It was in its waning gibbous phase on this day.

Figure 6.1

Image of the Lidar beam in the field of view of mCTI when looking at zenith

6.2 March 3

On this day I started my 5-second exposures at 8:41 PM and ended at 10:40 PM. ALE was still in my field of view so I offset mCTI the same amount as on February 27 and aligned the telescope with the marks on the observing pier. This night started off as clear and cool (close to freezing), but towards the end of the observing run, I started to see some high clouds. At the end of the observing run I had 1168 exposures. Then I took my bias and dark exposures. During the night the moon never was visible during the observations. It was in its waning crescent phase.

6.3 March 7

At 9:39 PM I started exposing with ALE. I offset mCTI due to ALE being in my field of view and aligned mCTI on the observing pole as I had on the previous nights. I took my bias and dark

exposures as I had on the other nights. The night sky was clear except for a few high clouds and the temperature was very cold. I stopped the exposures at 11:55 PM and collected a total of 1430 exposures. This night was the night of the new moon.

6.4 March 19

This day I took my flat fields. The temperature was relatively warm because I started an hour before dusk. The sky was very clear. I started taking the flat fields at 6:42 PM with 30 second exposures and went till 8:21 PM. Most of these images were overexposed due to the brightness of the sky and were not used in the flat fielding of the images. mCTI was still aligned the same way it had been on the previous nights in order to not change the direction of viewing for future observing.

6.5 March 21

On this night there was a full moon. Also, there were a lot of high clouds and airplane contrails floating over the field of view. I started exposing at 9:19 PM with ALE running alongside mCTI. The temperature was fairly warm that night, with a light wind. I finished exposing at 11:23 PM and then I took my bias and dark exposures. I collected 1203 exposures that night.

7. Data Reduction

While the continuous operation of mCTI creates a lot of data, the observing cadence and integration time limits the number of stars detected and useful for transparency measurements per frame. We could thus use standard astronomical data reduction systems for reducing data and extracting integrated fluxes for each star. Maxim DL was used for data acquisition and instrumental signature removal. Source Extractor is used for the photometry of individual star images. Matlab is used for the science data analysis and calculation of transparency as a function of time.

7.1 Source Extractor

To analyze the data that I recorded during my observation runs I had Maxim perform the canonical flat fielding and dark bias subtraction from all of my images. To extract the star information from each image I used Source Extractor [10].

Source Extractor used the Tycho-2 Catalogue [11] to extract a name for each point it thought was a star on my image. Also, for each star it extracted, it recorded a photon count using 5 different apertures and their associated error, the Cartesian coordinates of the position of the center of the star in pixels on the CCD chip, and also the right ascension and declination of the object. The background noise count was also recorded. If the star that Source Extractor was analyzing was partially out of the field of view or a number of other recurring problems were present, it would record a flag for that image.

Due to the massive volume of images that I would have to have manually put into Source Extractor, my colleague Pete Zimmer created an algorithm in Matlab that ran Source Extractor. This algorithm optimized the number of stars Source Extractor found, by changing many of the settings given to the program. The algorithm would then output a file with all of the data fields described for every star in every image.

7.2 Matlab

After I acquired my data fields, I was able to use Matlab to analyze the enormous amounts of data I received. I wrote a script that would take all of the individual star data for each night and group all the stars that had the same catalog number. If any of those points had flags associated with them, the script would delete them. It would then add the intensity counts for one minute together and add the error in quadrature over the same amount in time. To keep my results in the sub 1% range, the program would ignore any star that had a signal to noise ratio of less than 100 in one minute, which was at an approximate V magnitude of 9.

To calculate the extinction I used the equation:

$$S(t) = \int F(t,\lambda) \cdot T(t,\hat{z},\lambda) \cdot A \cdot I(t,\lambda)d\lambda$$

S(t) is the total photon flux detected, F is the spectral photon distributions of the sky and all sources present, $I(\lambda,t)$ is the instrumental transmission, A is the effective collecting area of the system, and $T(t,\hat{z},\lambda)$ is the atmospheric transmission in the $\hat{z}$ direction, averaged over the exposure time [7]. Since I am working in close to monochromatic light, the integral didn't have to be taken. Finding out the spectral photon distribution for each star was also beyond the scope of the project [7], so the Tycho catalog V magnitude would have to do.

In order to calculate transmittance of the atmosphere, I had to assume an average brightness of each star, which was taken from the Tycho V magnitude, and converted to intensity expected at the top of the atmosphere in a 2" aperture. The star photon count was normalized using its catalog intensity using this formula;

$$T_{atm}(t,\hat{z},\lambda) = \frac{S(t)}{S_{Star}(t)}$$

where S(t) is the photon flux received by mCTI and $S_{star}(t)$ is the flux from the star. To find the flux from each star in my field of view I assumed that the magnitudes given in the Tycho-2 catalog compiled by Høg [11], gave the total intensity of photons from the star. The mean error for the V magnitude of Tycho-2 stars is 0.013 magnitudes, so by using several stars per time resolved extinction measurement, we achieve the sub-1% measurement precision goal. Though the Tycho-2 V bandpass is broader than our filter bandpass, our bandpass is entirely contained within the V band and using this magnitude is justified for our purposes.

8. Results

The results derived from mCTI are very promising. Two of the nights show a strong correlation with the transmission acquired from ALE, while the other nights did not.
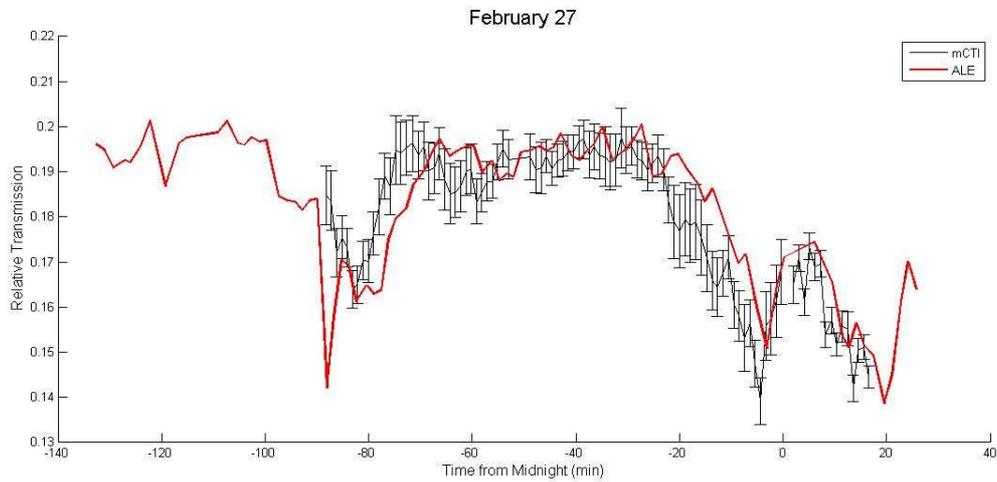
8.1 February 21st

Figure 8.1

Transmittance from February 21

In this figure we can see that ALE and mCTI's clocks were not exactly aligned correctly. Even though theses two images are slight shifted there is strong correlations between when the transmittance of the atmosphere was low and detected by both instruments.
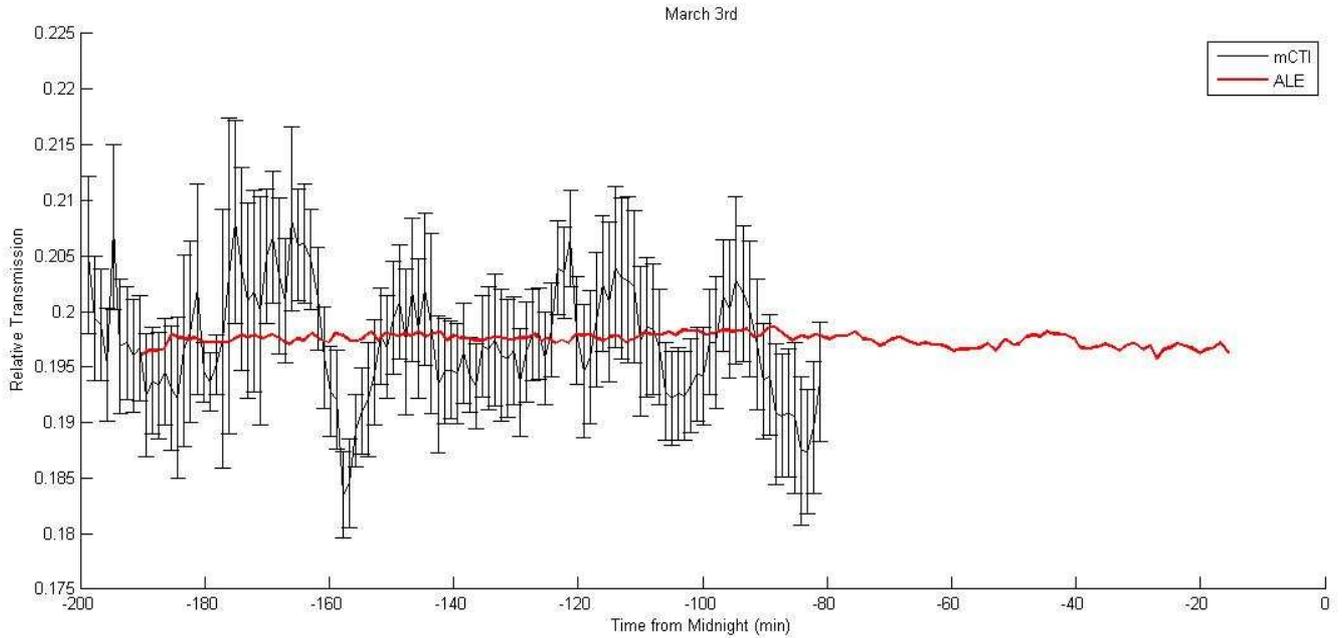
8.2 March 3rd

Figure 8.2

Transmittance from March 3rd

ALE's transmittance curve shows that this night was relatively clear. Looking at mCTI's curve shows a different story. These different light curves are still unknowns at the time. There are still many systematic errors inherent in both mCTI and ALE that need to be looked into and can be seen by looking at Figure 8.2.
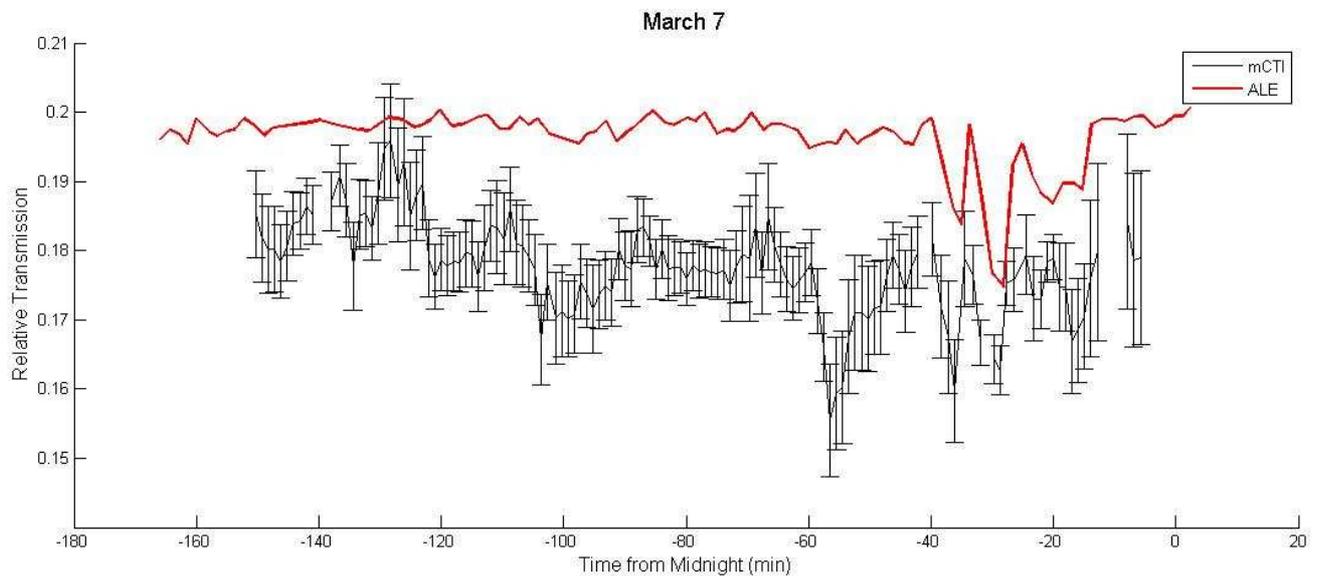
8.3 March 7th

Figure 8.3

Transmittance from March 7th

The variations from mCTI don't always match up with ALE. Then towards the end of the observing run both ALE and mCTI recorded a major change in the transmittance. On this night the relative transmission of mCTI was also lower than the other nights. This difference may be cause by systematic errors that will require more observations in order to determine them.
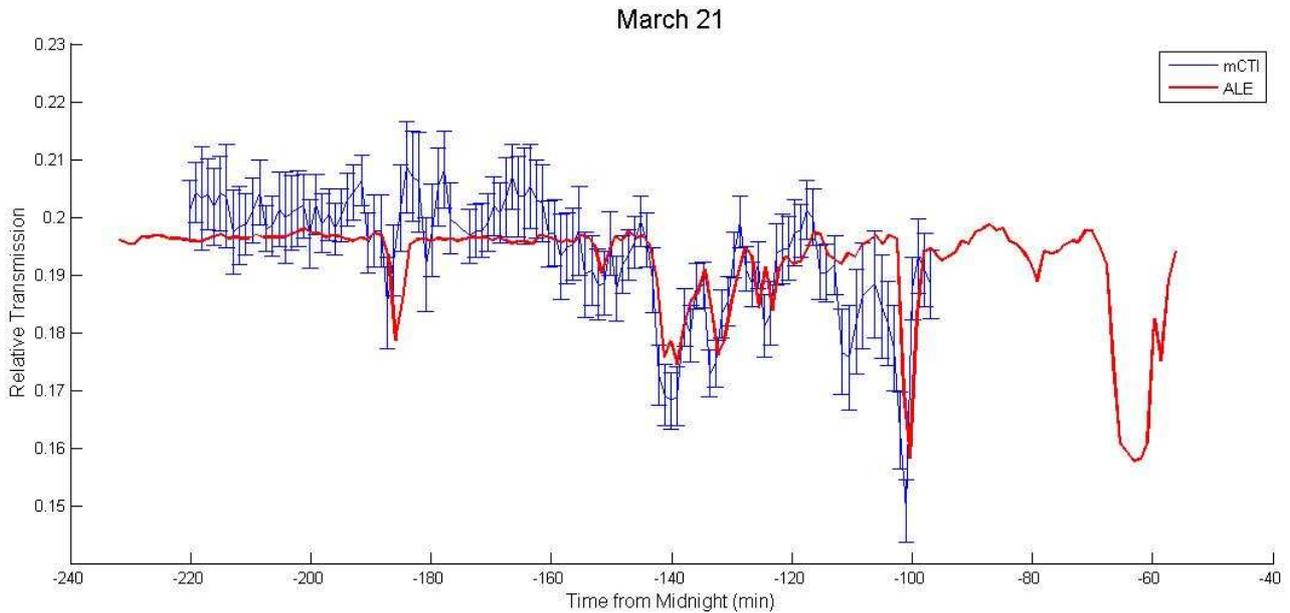
8.4 March 21st

Figure 8.4
Transmittance from March 21st

This night was a fairly turbid night and both ALE and mCTI confirm it. Some of the places where mCTI recorded lower transmittance than ALE may be errors due to the mismatch of the stars to the catalog. Overall, there are strong correlations here.

9. Summary and Future Work

This thesis addressed the beginning of successful calibration of ALE, which is a technology produced in order to help bring sub-1% photometric measurements to CTI-II and the rest of the astronomical community. Before mCTI was built, it was modeled so that the right parts could be acquired. Originally, mCTI was designed to run in TDI mode, but this method turned out to be too difficult to implement due to alignment problems, and it had too many problems associated with the differential drift time of the SBIG ST-402ME. The filters used in mCTI also caused problems due to their intrinsic property of producing ghost images. The mount was carefully selected to make mCTI easy to align with North when running in TDI mode, and be able to point

close to zenith when the Lidar was in the field of view. The problems encountered in designing and building mCTI were all overcome, resulting in an instrument that functions as planned.

mCTI observed in conjunction with ALE on four nights. Though this wasn't enough time to give good statistics of each star, it still produced enough data to compute the relative transmission accurately. The data was extracted from each image using Source Extractor and organized and analyzed using Matlab. These plots showed that ALE and mCTI exhibit a strong correlation in finding the transmission of the atmosphere on two nights. In order figure out why two of the observations between mCTI and ALE don't always match, more observations are needed. The observations will also help drive the error down in the standard photon flux of each star observed. That is needed to calculate the transmission of the atmosphere. Once the confidence of knowing the exact photon flux of each star is sufficient, these photon fluxes can be compared to the Tycho-2 catalogue list.

During the calculations of transmission for mCTI, it was noticed that not only was there a change in transmission across the whole field of view; there were also small transparency variations on the scale of the field. This leads to another direction that mCTI could take once the standard stars have been calibrated. We can potentially use mCTI to look for the angular differential transmission that happens in a large field of view. If the differential transmission could be accounted for in an image, this could help lead to even more precise astronomy.

Further along mCTI will likely be replaced by cCTI (centi-CTI) or dCTI (deci-CTI), larger collecting area and better detectors can ensure that many more stars can be imaged at a high signal to noise. This would allow far more detailed analysis including spatial and color variation. All of the preceding work in this thesis is directly applicable to such projects.

10. Acknowledgments

I would like thank Pete Zimmer for his patience, his advice, insight, and encouragement. Also I would like to thank John McGraw, for pushing me to do my best work.

References

1. McGraw, J.T., Ackermann, M. R., Williams, T., Zimmer, P., Walter, G., 2007 AAS/AAPT Joint Meeting, American Astronomical Society Meeting 209, #22.11; Bulletin of the American Astronomical Society, Vol. 38, p.930
2. Private communications with Pete Zimmer, 2007-08
3. Bodhaine, B.A., Mendonca, B. G., Harris, J. M., and Miller, J. M., Aug. 20, 1981, Journal of Geophysical Research, Vol. 86, NO. c8, P 7395-7398.
4. Stubbs, C. W. High, F. W., George, M. R., DeRose, K. L., Dlondin, S., Tonry, J. L., Chambers, K. C., Granett, B. R., Bulrne, D. L., Smith, R. C., Accepted PASP 2007 - http://arxiv.org/abs/0708.1364
5. Dawsey, M., Gimmestad, G., Roberts, D., McGraw, J., Zimmer, P., 2006, Volume 6270, pp. 62701F.
6. Private communications with John McGraw, 2007-08
7. Stubbs, Christopher W., and Tonry, John L., 12 Apr 2006, arXiv:astro-ph/0604285v1.
8. http://www.sbig.com/products/402_new.htm
9. http://shop.mellesgriot.com/products/optics/optics.asp?plga=044352&CatID=1014&mscssid= use
10. Bertin, E. and Arnouts, S., 1996, A&AS..117..393B.
11. Høg, E., Fabricius, C., Makarov, V. V., Urban, S., Corbin, T., Wycoff, G., Bastian, U., Schwekendiek, P. and Wicenec, A., 2000, A&A, 355: 27.
12. http://www.ccd.com/ascent_a98.html
13. http://www.ccd.com/ascent_a1107.html
14. Young, Andrew T, February 2, 1994, Applied Optics, Vol. 33 No. 6 p.1108.
15. Young, Andrew T., Genet, Russell M., Boyd, Louis J., Borucki, Willam J., Lockwood, G. Wesley, Henry, Gregory W., Hall Douglas S., Smith, Diane P., Baliunas, Sallie L., Donahue, Robert, and Epand, Donald H., February 1991, Astronomical Society of the Pacific, 103: 221-242.
16. Smalley, Barry, Gulliver, Austin F. and Adelman, Saul J., 2007, THE FUTURE OF PHOTOMETRIC, SPECTROPHOTOMETRIC AND POLARIMETRIC STANDARDIZATIONASP Conference Series, Vol. 999.
17. Young, A. T., 1974 May 1, The Astrophysical Journal, 189:587-604.
18. http://www.grida.no/climate/ipcc_tar/wg1/168.htm